HHS Public Access

Author manuscript

Nanomedicine. Author manuscript; available in PMC 2018 October 01.

Published in final edited form as:

Nanomedicine. 2017 October ; 13(7): 2359–2369. doi:10.1016/j.nano.2017.06.014.

Uptake of dendrimer-drug by different cell types in the hippocampus after hypoxic-ischemic insult in neonatal mice: effects of injury, microglial activation and hypothermia

Christina L. Nemeth[a,b], **Gabrielle T. Drummond**[a], **Manoj K. Mishra**[c], **Fan Zhang**[c], **Patrice Carr**[a], **Maxine S. Garcia**[a], **Sydney Doman**[a], **Ali Fatemi**[a,b], **Michael V. Johnston**[a,b], **Rangaramanujam M. Kannan**[a,c], **Sujatha Kannan**[a,d], and **Mary Ann Wilson**[a,b,e]

[a]Hugo W. Moser Research Institute at Kennedy Krieger, 707 N Broadway, Baltimore, MD 21205, USA

[b]Department of Neurology, The Johns Hopkins University School of Medicine, 1800 Orleans St., Baltimore, MD 21287, USA

[c]Center for Nanomedicine at the Wilmer Eye Institute, The Johns Hopkins University School of Medicine, 400 N Broadway, Baltimore, MD 21287, USA

[d]Anesthesiology and Critical Care Medicine, The Johns Hopkins University School of Medicine, The Charlotte R. Bloomberg Children's Center, 1800 Orleans Street, Suite 6318D, Baltimore, MD 21287, USA

[e]Department of Neuroscience, The Johns Hopkins University School of Medicine, 725 N. Wolfe St., Baltimore, MD 21205, USA

Abstract

Perinatal hypoxic-ischemic encephalopathy (HIE) can result in neurodevelopmental disability, including cerebral palsy. The only treatment, hypothermia, provides incomplete neuroprotection. Hydroxyl polyamidoamine (PAMAM) dendrimers are being explored for targeted delivery of therapy for HIE. Understanding the biodistribution of dendrimer-conjugated drugs into microglia, neurons and astrocytes after brain injury is essential for optimizing drug delivery. We conjugated N-acetyl-L-cysteine to Cy5-labeled PAMAM dendrimer (Cy5-D-NAC) and used a mouse model of perinatal HIE to study effects of timing of administration, hypothermia, brain injury, and microglial activation on uptake. Dendrimer conjugation delivered therapy most effectively to activated microglia but also targeted some astrocytes and injured neurons. Cy5-D-NAC uptake was

Correspondence to: Sujatha Kannan; Mary Ann Wilson.

Competing interests: RMK and SK are co-founders and shareholders of Ashvattha Therapeutics, LLC and Orpheris Inc., which are working towards the commercial translation of the dendrimer platform technologies. The Johns Hopkins University and Kennedy Krieger Institute have applied for patents related to the present work in which RMK, SK, MKM, FZ, AF, MVJ and MAW are inventors.

Prior presentation of abstracts regarding this research: Society for Neuroscience Annual Meeting and Baltimore Chapter Meeting 2015, Pediatric Academic Societies Meeting 2015, Hershey Conference on Developmental Brain Injury 2016

correlated with brain injury in all cell types and with activated morphology in microglia. Uptake was not inhibited by hypothermia, except in CD68+ microglia. Thus, dendrimer-conjugated drug delivery can target microglia, astrocytes and neurons and can be used in combination with hypothermia for treatment of HIE.

Graphical abstract

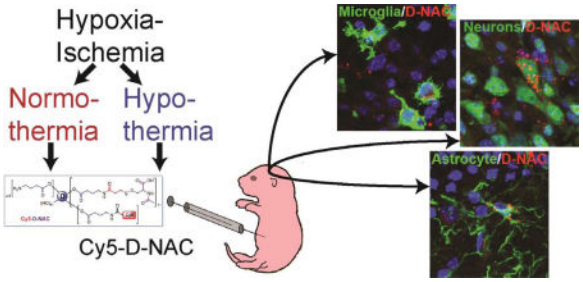

Hydroxyl polyamidoamine dendrimers are being explored for targeted delivery of therapy for hypoxic-ischemic encephalopathy. We examined cellular uptake of N-acetyl-L-cysteine conjugated to Cy5-labeled dendrimer in a neonatal mouse model of hypoxic-ischemic encephalopathy, with or without therapeutic hypothermia. Dendrimer conjugation delivered therapy most effectively to activated microglia but also targeted astrocytes and injured neurons. Uptake correlated with brain injury and with activated morphology in microglia. Uptake was not impaired by hypothermia, except in CD68+ microglia; thus, dendrimer delivery can be combined with therapeutic hypothermia.

Keywords

Hypoxia-ischemia; cerebral palsy; dendrimer nanoparticles; microglia; hypothermia; neuroinflammation

Background

Understanding *in vivo* interactions between nanomaterials and disease pathology can provide valuable insights for designing new drug delivery systems. If such interactions can be harnessed for superior drug delivery, without complex ligand targeting strategies, it may enable simple constructs that may be easier to translate. Prior studies with hydroxyl polyamidoamine (PAMAM)† dendrimers showed that they can selectively localize in injured glial cells, following systemic administration in models of brain injury. However, detailed characterization of the biodistribution of dendrimers in different cells in the brain as injury progresses, and as an effect of the severity of injury, are still not well explored.[1,2] This study investigates these effects within the context of neonatal brain injury.

†Abbreviations: PAMAM: polyamidoamine, HIE: hypoxic-ischemic encephalopathy, NAC: N-acetyl-L-cysteine, D-NAC: dendrimer-NAC conjugate, D-Cy5: Cy5-labeled dendrimer, Cy5-D-NAC: Cy5-labeled dendrimer-NAC conjugate, P: postnatal day; M: Male, F: Female NeuN: neuronal nuclei, GFAP: glial fibrillary acidic protein, Iba1: ionized calcium binding adapter molecule 1, DG: dentate gyrus, CA: cornu ammonis region of hippocampus

Neonatal hypoxic-ischemic encephalopathy (HIE) occurs in approximately 2/1000 births and can lead to a range of neurodevelopmental disabilities including cerebral palsy.[3,4] The etiology of HIE is highly variable, arising from a sentinel event occurring late in pregnancy or in the intrapartum period.[5,6] Infants that suffer a hypoxic-ischemic (HI) insult often exhibit severe lethargy, seizures, hypotonia, and poor feeding during the neonatal period, with brain injury detectable by high resolution imaging within the first few hours of life.[5,7] Brain injury is thought to begin with primary energy failure in neurons and astrocytes that drives glutamate release and excitotoxic injury, and progresses towards a second surge of cell death after 24 hours.[3,8] Inflammatory processes begin within a few hours of injury and can last for weeks, contributing to delayed neuronal death and injury progression.[4,9] Glutamate and inflammatory cytokines trigger multiple injury pathways that result in a continuum of apoptotic, necroptotic, and necrotic cell death.[10–12] Therapeutics aimed at these pathways may slow cell death and inflammatory processes, reduce overall injury, and provide a platform for recovery.

Therapeutic hypothermia remains the primary treatment option for infants with HIE because it reduces mortality and brain injury, resulting in better neurological outcomes.[3,13–15] Hypothermia acts on several different pathways, reducing metabolic demand[16] and glutamate release, suppressing inflammation,[11,17,18] mitigating dysfunction of ion pumps, and interfering with apoptotic pathways.[19,20] Timing and intensity of cooling are critical; preclinical evidence shows that delayed cooling and over-cooling negatively correlate with neuroprotection.[3] Despite the benefits of therapeutic hypothermia, neuroprotection is incomplete[3,13,21] and combination therapies are needed.[22–24]

New strategies in nanomedicine can improve the bioavailability and targeting of existing approved drugs, which may improve efficacy. *N*-acetyl-L-cysteine conjugated to generation-4 hydroxyl (G4-OH) PAMAM dendrimer (D-NAC) is a promising candidate for treatment of HI and inflammatory brain injury. D-NAC has been shown to reduce white matter injury following murine neonatal ischemia[25] and to reduce cerebral inflammation and improve motor function in a rabbit maternal inflammation model of cerebral palsy.[26] Importantly, these previous studies also demonstrate that conjugation of drugs to PAMAM dendrimer facilitates localization to, and uptake by, cells involved in inflammation, while restricting uptake by normal cells.[25] However, therapeutic hypothermia has been widely adopted as therapy for HIE, and it is therefore important to determine whether hypothermia alters D-NAC brain localization and uptake after HI.

Previous studies using hydroxyl PAMAM dendrimer in mouse, rat, rabbit, canine, and primate models focused on the ability of Cy5-labeled dendrimer (D-Cy5) to target inflammation. In this study, we assess whether NAC-conjugated dendrimer-Cy5 (Cy5-D-NAC) targets injured brain cells. To do this, we quantitatively assessed the cellular biodistribution of Cy5-D-NAC within neurons, astrocytes, and microglia in a neonatal mouse model of HI, with or without therapeutic hypothermia. We focused our analysis in the hippocampus, a region that is highly sensitive to neonatal HI, exhibiting both apoptotic and necrotic cell death,[27] and which we found is protected by therapeutic hypothermia. Our objectives were to determine if dendrimer uptake is altered by hypothermia, whether the

timing of Cy5-D-NAC treatment alters uptake in these cell types, and if the observed cellular localization is consistent with that observed in other models of brain injury.

Methods

Sources for antibodies, materials and equipment are shown in Supplementary Table S1.

Preparation of Cy5-labeled D-NAC conjugate

The bifunctional dendrimer was prepared following an established protocol[26,28] and was then reacted with Cy5, followed by reaction of linker and NAC in two steps. This synthetic procedure is described in Supplementary Materials (Figure S1).

Animals and surgical procedure

The experimental design is diagrammed in Figure 1. Animal procedures were carried out in accordance with the National Institutes of Health Guide for the Care and Use of Laboratory Animals and approved by the Institutional Animal Care and Use Committee of Johns Hopkins University. Ten lactating female CD-1 mice with litters of 10 pups were obtained at postnatal day (P) 6 (day of birth = P1, Charles River Laboratories). On P7, 4 male and 4 female pups per litter were anesthetized and the right common carotid artery was permanently ligated. Pups recovered 75–90 minutes at 36 °C before hypoxia (10% O_2, balance N_2, 36 °C, 15 min). Further details are in Supplemental Methods.

Immediately following HI, mice were randomized to 6 h of normothermia (ambient 36.5 °C) or hypothermia (ambient 30.5 °C), with 2 males and 2 females per litter in each temperature group. Remaining mice served as uninjured controls. Pups were placed in individual chambers on an aluminum platform within an incubator. Pilot studies showed that 7 days after HI, brain injury was less severe in hypothermic mice (Supplementary Figure S2; $p < 0.05$) and body temperatures stabilized within 20 min and remained at ~33 °C in the hypothermic group and ~36.5 °C in the normothermic group for the 6 h period of hypothermia/normothermia. Therefore, in the present study, incubator temperatures were set at 30.5 °C and 36.5 °C for hypothermia and normothermia, respectively, and monitored throughout. Core body temperature was monitored 30 min and 6 h after HI (mean at 6 h: 31.6 °C and 35.4 °C).

To determine the effect of injection time on uptake of D-NAC, mice were injected with Cy5-D-NAC (10 mg/kg; *i.p.*) at 0, 6, or 24 h after HI (Table 1). Dendrimer-conjugated NAC has been extensively tested for *in vivo* safety and stability; this dose has resulted in both cellular uptake and functional recovery in neonatal models of ischemic and inflammatory brain injury.[25,26] Mice were perfused with 10% formalin, 24 h after injection of Cy5-D-NAC (24, 30, or 48 h after HI). Brains were post-fixed 4 h, cryoprotected, and frozen.

Immunohistochemical labeling of microglia, neurons, and astrocytes

Brains were sectioned (20 μm) and 1 in 6 series of coronal sections throughout the forebrain were stained with cresyl-violet to evaluate histopathology or processed for immunohistochemical labeling of microglia, neurons, or astrocytes. Sections were incubated

with primary antibodies for Iba1 (ionized calcium binding adapter molecule 1), NeuN (neuronal nuclei), GFAP (glial fibrillary acidic protein), or CD68, followed by secondary antibody conjugated to Alexa Fluor® 488 (Supplementary Table S1). For GFAP, sections were pretreated with L.A.B. solution for 30 min at 60 °C for antigen retrieval. Sections were counterstained with DAPI, coverslipped with DAKO fluorescence mounting medium, and stored at −20 °C.

Injury assessment

Cresyl-violet-stained sections were assessed for neuropathology (Supplementary Figure S3) and injury was scored as follows: 0) no apparent injury; 1) mild injury, small groups of pyknotic cells (condensed nuclei) within the hippocampus; 2) moderate injury, larger groups of injured cells or small areas of infarction within the hippocampus and other regions (cortex, striatum, or thalamus); 3) severe injury, extensive confluent infarction or tissue cavitation.

Analysis of dendrimer uptake

In the contralateral, uninjured hemisphere of mice subjected to HI or in brains of uninjured control mice, Cy5-D-NAC was not detected outside blood vessels; quantitative analysis of dendrimer uptake was therefore limited to the ligated hemisphere. Due to its vulnerability to HI injury, the hippocampus was selected for uptake analysis. For quantification of uptake in each cell type, nine microscopic fields located within CA1, CA3, or DG in three sections of dorsal hippocampus from each animal (Supplementary Figure S4) were imaged and evaluated. Fluorescence images were captured with a Zeiss Axio Imager M2 microscope with consistent imaging settings using a 40× objective for neurons (NeuN), astrocytes (GFAP), and phagocytic microglia (CD68) or a 20× objective for microglia (Iba1). Cells containing each marker and a DAPI-stained nucleus were counted and evaluated for Cy5-D-NAC labeling in z-stack images from each subject by investigators blinded to experimental group, using AxioVision 4.8.2 (Zeiss), and the proportion of these cells co-labeled with Cy5-D-NAC was calculated. Because injury mechanisms vary among hippocampal regions, uptake was examined in images from each region.

Evaluation of microglial morphology

Microglial morphology was examined as an indicator of activation, in the same images used for analysis of microglial uptake. Each set of z-stack images from CA1, CA3, or DG was examined by two investigators blinded to experimental group. Microglial morphology was classified as ramified (small soma with thin, finely branching processes), moderately activated (enlarged soma with thickened, sometimes sheet-like processes), or highly activated (ameboid, with a large rounded soma and few/no processes). A score was assigned according to the predominant cell type or mixture observed: 1) nearly all cells ramified; 2) a mixture of ramified and moderately activated morphology; 3) nearly all cells with moderately activated morphology; 4) a mixture of cells with moderately activated and ameboid morphology; or 5) nearly all cells with ameboid morphology. Scores assigned in CA1, CA3, and DG by both raters were averaged to obtain a microglial activation score for the hippocampus in each animal.

Data analysis

Statistical analyses were completed using IBM SPSS Statistics 23. No differences in dendrimer uptake were detected between males and females; therefore, these data were collapsed by group. The effect of treatment on injury severity was analyzed using a Kruskal-Wallis test. For each cell type, the effect of injury severity on uptake was examined using Spearman's rank-order correlation. Hippocampal and subregion uptake data were analyzed by two-way ANCOVA with injection time and temperature as factors and injury score as covariate. Significant main effects and interactions were further evaluated by *a priori* contrast comparisons. For microglia, relationships between injury and morphology score and between morphology score and uptake were examined using Spearman's rank-order correlation. Findings were considered significant when $p \leq 0.05$.

Results

Preparation of Cy5 labelled dendrimer-NAC conjugate

Previously, dendrimer-*N*-acetyl-L-cysteine (D-NAC) was designed, synthesized, and validated for targeting neuroinflammation,[26,28] and dendrimer-Cy5 (D-Cy5) was prepared, characterized, and quantified in a neonatal rabbit model.[29,30] To prepare the novel conjugate, Cy5-D-NAC, for this dendrimer-drug uptake study in our neonatal hypoxic-ischemic mouse model, a modified synthetic scheme was followed. Our starting material consisted of a bifunctional G4-OH dendrimer with 17–18 amine groups on the surface of the hydroxyl dendrimer, so that the free amine groups would further react with NAC.[28] After reacting this bifunctional dendrimer with one molar equivalent of Cy5-mono-NHS-ester, we obtained Cy5-labeled dendrimer with more than 15 unreacted amine groups on the surface of the dendrimer. NAC was reacted with this intermediate using SPDP as a linker, and this produced D-NAC with disulfide linkage and labeled with Cy5. The resulting conjugate, Cy5-D-NAC, was purified by dialysis followed by GPC fractionation and was extensively analyzed by RP-HPLC, UV-vis spectrum, and ^{1}H-NMR. HPLC (Figure 2A) showed a peak at 28.1 min, distinct from that of the starting dendrimer and free Cy5, supporting a pure conjugate. The UV spectrum (Figure 2B) showed peaks characteristic of PAMAM dendrimer and Cy5; the percentage payload of Cy5 to dendrimer is approximately 5%. In the ^{1}H NMR spectrum (Figure 2C), multiplets were present at 1.24–1.53 ppm for CH_2 protons of the linker, a singlet at 1.86 ppm for acetyl protons of NAC, a multiplet at 4.47 for CH protons of NAC, and multiplets at 6.30–7.85 ppm for aromatic protons of Cy5 along with the peaks associated with dendrimer confirmed the formation of the conjugate. Loading of NAC was calculated using the proton integration method; 11 NAC molecules were reacted to the dendrimer to achieve drug loading of approximately 9.8% by weight.

Histopathology at 24 to 48 h after HI

Mice subjected to HI on P7 were euthanized 24 h after injection of Cy5-D-NAC (24, 30 or 48 h after HI). To determine whether cellular uptake is altered in response to initial brain injury, histopathology was scored in Nissl-stained sections. A regional pattern of injury in cortex, hippocampus, basal ganglia and thalamus that mimics cerebral damage observed in term infants with HIE was observed (Supplementary Figure S3). Histopathology ranged from no injury to severe injury within each treatment group. In contrast to the

neuroprotective effect of hypothermia observed 7 days after HI in the pilot study, at this early time point there were no differences among treatment groups (Kruskal-Wallis, p = 0.208).

Uptake of dendrimer by microglia

Cy5-D-NAC uptake was examined in the hippocampus at a consistent interval, 24 hours after injection. In the uninjured hemisphere of mice subjected to HI and in brains of uninjured controls, Cy5-D-NAC was not detected outside blood vessels. On the ligated side, Cy5-D-NAC was localized within microglia in each region of the hippocampus examined (Figure 3A). Because dendrimer conjugates are known to target activated microglia,[26,28] and microglial activation is stimulated by injury, we first examined the relationship between microglial uptake and brain injury. There was a significant correlation between microglial uptake of Cy5-D-NAC and brain injury score (Figure 3B, Spearman's rho = 0.62; $p < 0.01$). When covariate analysis was used to control for the degree of injury, we confirmed that injury significantly affected uptake of Cy5-D-NAC by microglia ($F_{1,71} = 55.83$, $p < 0.001$), and we found that microglial uptake varied as a function of injection time ($F_{2,71} = 7.16$, $p < 0.01$; estimated marginal means are depicted in Figure 3C). Moderate microglial uptake of Cy5-D-NAC was observed after injection at 0 or 6 h, but uptake was greater after injection at 24 h than at earlier time points (contrast analyses, $p < 0.01$ for each). Thus, the interval between HI and Cy5-D-NAC treatment is an important determinant of uptake by microglia. Because timing and mechanisms of cell injury vary among hippocampal regions, independent covariate analysis was conducted in CA1, CA3, and DG. As observed overall, injury affected microglial uptake within each region (CA1: $F_{1,71} = 28.40$, $p < 0.001$; CA3: $F_{1,71} = 43.29$ $p < 0.001$; DG: $F_{1,71} = 43.34$, $p < 0.001$). The temporal pattern of uptake in each region resembled the overall pattern of uptake in the hippocampus, with a significant effect of injection time in DG (Supplementary Figure S5; $F_{2,71} = 7.01$, $p < 0.05$) and a trend in CA3 ($F_{2,71} = 2.76$, $p = 0.07$). In DG, most cell death after HI is apoptotic, and microglial uptake was significantly greater after injection at 24 h than at 0 ($p < 0.01$) or 6 h ($p < 0.05$). Importantly, hypothermia did not alter dendrimer uptake into microglia.

The morphology of Iba1-labeled microglia was consistent with activation in response to hippocampal neuronal injury. Hippocampal microglia in controls exhibited a highly ramified morphology with a small soma (Figure 4A), but after HI, microglia in the hippocampus exhibited morphology characteristic of activation (Figure 4B–D) that varied with the degree of injury (Figure 4E, Spearman's rho = 0.73, $p < 0.001$). Microglial uptake of Cy5-D-NAC was strongly correlated with activation, as indicated by microglial morphology score (Figure 4F, Spearman's rho = 0.79, $p < 0.001$). In CD68+ phagocytic microglia, uptake correlated with injury (Figure 5B, Spearman's rho = 0.514, $p < 0.01$), and uptake was greater than that observed in Iba1+ microglia ($p < 0.001$). In this subset of microglia, uptake was greater in normothermic animals than in hypothermic animals ($p < 0.05$).

Uptake of dendrimer by neurons

Cy5-D-NAC was detected in neurons within each region of the hippocampus after HI (Figure 6A); however, the proportion of neurons taking up Cy5-D-NAC was much less than the proportion of microglia taking up dendrimer. When the hippocampus was assessed as a

whole, dendrimer uptake varied with injury score ($F_{1,74} = 4.21$, $p < 0.05$), but the correlation was less robust than that observed in microglia (Figure 6B; Spearman's rho = 0.46, $p < 0.01$). After adjustment for the effect of injury, no effects of injection time or hypothermia were detected when hippocampal regions were pooled (estimated marginal means shown in Figure 6C). In contrast, when evaluated separately, a distinct pattern emerged in CA1, where neuronal uptake varied with injection time (Figure 7A; CA1: $F_{2,74} = 3.72$, $p < 0.05$). Uptake tended to be greater when Cy5-D-NAC was injected immediately after HI than at 6 h ($p = 0.07$), and uptake was greater when Cy5-D-NAC was injected at 24 h than at 6 h ($p < 0.05$). No differences were detected in CA3 (Figure 7B). However, in DG, neuronal uptake of Cy5-D-NAC increased with injury ($F_{1,74} = 11.17$, $p < 0.01$) and there was a significant interaction of injection time and temperature (Figure 7C; $F_{2,73} = 3.96$, $p < 0.05$). Within this region in hypothermic animals, neuronal uptake was greater when Cy5-D-NAC was injected 6 h after HI, at the onset of rewarming, than at 0 or 24 h ($p < 0.05$), and after injection at 6 h, there was greater uptake in hypothermic animals than in normothermic animals ($p < 0.05$).

Uptake of dendrimer by astrocytes

Due to their role in neuroinflammation and their potential as a therapeutic target, dendrimer conjugate localization within GFAP+ astrocytes was assessed. As in other cell types, Cy5-D-NAC was detected within astrocytes in each region of the hippocampus examined after injection at each time point (Figure 8A). As observed in microglia and neurons, astrocyte uptake of Cy5-D-NAC was affected by ($F_{1,65} = 12.22$, $p < 0.05$), and correlated with, HI injury (Figure 8B; Spearman's rho = 0.48, $p < 0.01$). When adjusted for injury and with hippocampal regions combined, no effects of injection time or temperature were detected (Figure 8C). When evaluated by region, patterns of uptake were similar and no effects of injection time or hypothermia were detected (Supplementary Figure S6).

Discussion

Nanotherapeutics offer new strategies for targeted treatment of HI brain injury. Our analysis of cellular uptake of Cy5-labeled D-NAC in a mouse model of HIE examined the effects of therapeutic hypothermia and time of administration on uptake, and we used a correlation analysis to examine the effects of brain injury and microglial activation on D-NAC uptake in this model. These results expand upon previous findings that support the use of dendrimer therapy for brain injury in other neonatal[25,26,30] and large animal models.[28]

Dendrimer-NAC uptake as a function of cell type in the injured brain

HI in P7 CD1 mice produces a regional pattern of gray matter injury that mimics cerebral damage observed in term infants with HIE, and mild hypothermia has modest therapeutic effects. In this mouse model, Cy5-D-NAC was detected within microglia, neurons, and astrocytes after a single dose administered immediately or up to 24 h after HI, but only in the injured hemisphere. Cy5-D-NAC was not detected outside blood vessels in uninjured control mice. Thus, conjugation of drugs to dendrimer nanoparticles can selectively target therapy to all three cell types involved in brain injury after HI, while limiting drug delivery to uninjured tissue. The disulfide-based drug conjugation used in this study minimizes drug release in circulation, but after uptake it permits fast and reliable glutathione-sensitive release of drug

within targeted cells, an important consideration in designing therapy for acute brain injury such as HIE.[28,31]

Dendrimer uptake after HI varies by cell type and may be influenced by the severity of disruption of the blood-brain barrier and the degree of cellular activity.[28,32] Cy5-D-NAC accumulation was correlated with severity of injury in all cell types evaluated; this is similar to the correlation of uptake with neurobehavioral disease severity observed in a rabbit model of maternal inflammation-induced cerebral palsy.[33] The proportional uptake of Cy5-D-NAC was greatest and the correlation between uptake and injury was strongest in microglial cells, which become phagocytic when activated by brain injury.[34–36] Microglia expressing the phagocytic marker CD68 exhibited very high levels of uptake, with over 80% uptake in most injured animals. These data suggest that uptake in microglia involves a phagocytic mechanism.[2,37,38]

After HI, activation of microglia occurs rapidly and leads to migration, release of proinflammatory mediators and excitatory amino acids, and phagocytosis of injured neurons.[11,39,40] As expected, microglial activation in this study was strongly correlated with brain injury. Zhang and colleagues[41] reported that ameboid microglia in newborn rabbit brain slices exposed *in utero* to maternal inflammation exhibited greater PAMAM dendrimer uptake *in vitro*, compared to slices from unexposed controls with less activated microglial morphology. A similar association between ameboid morphology and dendrimer uptake was noted in this model after dendrimer administration *in vivo*.[33] Here, we scored microglial morphology as an indicator of activation after HI and demonstrated that dendrimer uptake increases as microglial activation increases. In our analysis of dendrimer uptake at different post-HI injection times, we expected microglia to show greater uptake as the response to injury progressed. Microglial uptake was robust over the 24 h period examined but was greater after injection at 24 h than at earlier time points. Depending on activation state, microglia can have beneficial or deleterious effects on neuronal survival, and timing of interventions directed at microglia may be critical in determining efficacy. Because uptake was robust in microglia both acutely and 24 h after HI, timing of therapy may be adjusted for optimal efficacy.

Neurons are highly susceptible to damage following HI, and intracellular delivery of NAC by dendrimer conjugates maintains cysteine levels, which may provide neuroprotection. However, the proportion of neurons containing detectable Cy5-D-NAC was low (~2–4% on an average), compared to that in activated microglia and astrocytes. Intense neuronal activity, which occurs during seizures triggered by neonatal HI,[42,43] drives activity-dependent endocytosis for synaptic vesicle retrieval.[44] This mechanism may underlie the selective, injury-related uptake of Cy5-D-NAC by neurons. Neuronal injury mechanisms differ in hippocampal subpopulations and evolve over 24–48 h after injury[45,46]; distinct patterns of neuronal dendrimer uptake at different injection times in these regions may be related to differences in these mechanisms, timing, or severity of injury.

Astrocytes become activated within 24 h after HI and have neuroprotective effects, scavenging glutamate, free radicals, and other excitotoxic factors while releasing trophic factors that promote survival.[9,11,39,47] Astrocyte activity heavily influences survival of

neurons, and although astrocytes are susceptible to HI injury, their survival contributes directly to the regenerative capacity of the injured area.[39] Thus, dendrimer-mediated delivery of NAC to activated astrocytes and microglia is expected to promote neuronal survival, reduce injury, and improve neurobehavioral function. Further work is needed to determine the effects of D-NAC at longer intervals after injury.

Effect of hypothermia on dendrimer-NAC uptake

Therapeutic hypothermia can alter the disposition and metabolism of pharmacological interventions, resulting in altered clearance and higher rates of toxicity.[48–50] We thus expected that hypothermia might impair temperature-dependent dendrimer uptake mechanisms or delay excretion, prolonging the time in circulation.[11,19] However, uptake of Cy5-D-NAC in animals exposed to therapeutic hypothermia was largely similar to that in animals maintained in normothermic conditions, with only a small increase in neuronal uptake during rewarming in one region of the hippocampus, and a modest decrease in CD68+ microglia in hypothermic animals at early administration times. *In vitro* studies have shown that hydroxyl-terminated dendrimers are taken up by active fluid phase pinocytosis and that uptake is inhibited at 10 °C.[37,51] The body temperature used for therapeutic hypothermia (~33 °C) did not impair uptake in most microglia, but may slow phagocytosis during hypothermia and rewarming.

The *in vivo* interactions between dendrimer nanoparticles and the severity and progression of brain injury reported here provide valuable insights for the design and implementation of new drug delivery systems. We have shown that uptake of systemically delivered dendrimer-conjugated drug is correlated with injury in all three cell types examined and with activation in microglia. Thus, dendrimer conjugation can selectively deliver therapy to injured brain regions, limit delivery to uninjured tissue, and can effectively target activated microglia and injured cells. This specific targeting of therapy may improve drug efficacy and limit adverse drug effects. We have confirmed that dendrimer conjugation is most effective for delivery of therapy to activated microglia, but we show that it can also target activated astrocytes and injured neurons. Timing of therapy can be adjusted to achieve optimal efficacy, because uptake was similar after administration 0, 6, or 24 h after HI. Our most important finding regarding clinical therapy for HIE, in which hypothermia has been adopted as standard care, is that dendrimer-drug uptake was generally not impaired by hypothermic treatment. These findings demonstrate that in a murine model of neonatal HIE, dendrimer conjugate treatment can be used to selectively deliver therapy to injured brain regions when administered immediately after injury or with a delay, and dendrimer conjugation can effectively target drug delivery for hypoxic-ischemic brain injury in combination with the current standard of care, hypothermia.

Supplementary Material

Refer to Web version on PubMed Central for supplementary material.

Acknowledgments

Research reported in this publication was supported by the National Institute of Child Health and Human Development of the National Institutes of Health under award numbers U54HD079123 (MAW, SK), T32HD007414 (CLN), and R01HD076901 (RMK), and by the Cerebral Palsy Foundation (AF, MVJ, SK, RMK). The statistical analysis received support from the National Center for Research Resources and the National Center for Advancing Translational Sciences (NCATS) of the National Institutes of Health under award number 1UL1TR001079. The content is solely the responsibility of the authors and does not necessarily represent the official views of the National Institutes of Health.

References

1. Zhang F, Lin YA, Kannan S, Kannan RM. Targeting specific cells in the brain with nanomedicines for CNS therapies. J Control Release. 2015; 240:212–26. DOI: 10.1016/j.jconrel.2015.12.013 [PubMed: 26686078]
2. Kannan RM, Nance E, Kannan S, Tomalia DA. Emerging concepts in dendrimer-based nanomedicine: From design principles to clinical applications. J Int Med. 2014; 276:579–617. DOI: 10.1111/joim.12280
3. Davidson JO, Wassink G, van den Heuij LG, Bennet L, Gunn AJ. Therapeutic hypothermia for neonatal hypoxic–ischemic encephalopathy – where to from here? Front Neurol. 2015; 6:198.doi: 10.3389/fneur.2015.00198 [PubMed: 26441818]
4. Bhalala US, Koehler RC, Kannan S. Neuroinflammation and neuroimmune dysregulation after acute hypoxic-ischemic injury of developing brain. Front Pediatr. 2015; 2:144.doi: 10.3389/fped.2014.00144 [PubMed: 25642419]
5. Fatemi A, Wilson MA, Johnston MV. Hypoxic-ischemic encephalopathy in the term infant. Clin Perinatol. 2009; 36:835–58. DOI: 10.1016/j.spen.2009.09.001 [PubMed: 19944838]
6. Okereafor A, Allsop J, Counsell S, Fitzpatrick J, Azzopardi D, Rutherford M, et al. Patterns of brain injury in neonates exposed to perinatal sentinel events. Pediatrics. 2008; 121:906–14. [PubMed: 18450893]
7. Schaefer PW, Grant PE, Gonzalez RG. Diffusion-weighted MR imaging of the brain. Radiology. 2000; 217:331–45. DOI: 10.1148/radiology.217.2.r00nv24331 [PubMed: 11058626]
8. Descloux C, Ginet V, Clarke PGH, Puyal J, Truttmann AC. Neuronal death after perinatal cerebral hypoxia-ischemia: Focus on autophagy—mediated cell death. Int J Dev Neurosci. 2015; 45:75–85. DOI: 10.1016/j.ijdevneu.2015.06.008 [PubMed: 26225751]
9. Burtrum D, Silverstein F. Hypoxic-ischemic brain injury stimulates glial fibrillary acidic protein mRNA and protein expression in neonatal rats. Exp Neurol. 1994; 126:112–8. DOI: 10.1006/exnr.1994.1047 [PubMed: 8157121]
10. Chavez-Valdez R, Martin LJ, Northington FJ. Programmed necrosis: A prominent mechanism of cell death following neonatal brain injury. Neurol Res Int. 2012; 2012:257563.doi: 10.1155/2012/257563 [PubMed: 22666585]
11. Hagberg H, Mallard C, Ferriero DM, Vannucci SJ, Levison SW, Vexler ZS, et al. The role of inflammation in perinatal brain injury. Nat Rev Neurol. 2015; 11:192–208. DOI: 10.1038/nrneurol.2015.13 [PubMed: 25686754]
12. Northington FJ, Chavez-Valdez R, Martin LJ. Neuronal cell death in neonatal hypoxia-ischemia. Ann Neurol. 2011; 69:743–58. DOI: 10.1002/ana.22419 [PubMed: 21520238]
13. Silveira RC, Procianoy RS. Hypothermia therapy for newborns with hypoxic ischemic encephalopathy. J Pediatr. 2015; 91:S78–83. DOI: 10.1016/j.jped.2015.07.004
14. Jacobs S, Berg M, Hunt R, Tarnow-Mordi W, Inder T, Davis P. Cooling for newborns with hypoxic ischaemic encephalopathy. Cochrane Database Syst Rev. 2013; :1–112. DOI: 10.1203/00006450-200508000-00210
15. Shankaran S. Outcomes of hypoxic-ischemic encephalopathy in neonates treated with hypothermia. Clin Perinatol. 2014; 41:149–59. DOI: 10.1016/j.clp.2013.10.008 [PubMed: 24524452]
16. Wisnowski JL, Wu T-W, Reitman AJ, McLean C, Friedlich P, Vanderbilt D, et al. The effects of therapeutic hypothermia on cerebral metabolism in neonates with hypoxic-ischemic

encephalopathy: An in vivo 1 H-MR spectroscopy study. J Cereb Blood Flow Metab. 2016; 35:1075–86. DOI: 10.1177/0271678X15607881

17. Jenkins DD, Lee T, Chiuzan C, Perkel JK, Rollins LG, Wagner CL, et al. Altered circulating leukocytes and their chemokines in a clinical trial of therapeutic hypothermia for neonatal hypoxic ischemic encephalopathy. Pediatr Crit Care Med. 2013; 14:786–95. DOI: 10.1097/PCC.0b013e3182975cc9 [PubMed: 23897243]
18. Chakkarapani E, Davis J, Thoresen M. Therapeutic hypothermia delays the C-reactive protein response and suppresses white blood cell and platelet count in infants with neonatal encephalopathy. Arch Dis Child Fetal Neonatal Ed. 2014; 99:F458–63. DOI: 10.1136/archdischild-2013-305763 [PubMed: 24972990]
19. Schmitt K, Tong G, Berger F. Mechanisms of hypothermia-induced cell protection in the brain. Mol Cell Pediatr. 2014; 1:1–5. DOI: 10.1186/s40348-014-0007-x [PubMed: 26567095]
20. Takenouchi T, Sugiura Y, Morikawa T, Nakanishi T, Nagahata Y, Sugioka T, et al. Therapeutic hypothermia achieves neuroprotection via a decrease in acetylcholine with a concurrent increase in carnitine in the neonatal hypoxia-ischemia. J Cereb Blood Flow Metab. 2015; 35:794–805. DOI: 10.1038/jcbfm.2014.253 [PubMed: 25586144]
21. Ek CJ, D'Angelo B, Baburamani AA, Lehner C, Leverin A-L, Smith PL, et al. Brain barrier properties and cerebral blood flow in neonatal mice exposed to cerebral hypoxia-ischemia. J Cereb Blood Flow Metab. 2015; 35:818–27. DOI: 10.1038/jcbfm.2014.255 [PubMed: 25627141]
22. Shankaran S. Therapeutic hypothermia for neonatal encephalopathy. Curr Opin Pediatr. 2015; 27:152–7. DOI: 10.1007/s11940-012-0200-y [PubMed: 25689454]
23. Burnsed JC, Chavez-Valdez R, Hossain MS, Kesavan K, Martin LJ, Zhang J, et al. Hypoxia-ischemia and therapeutic hypothermia in the neonatal mouse brain - a longitudinal study. PLoS One. 2015; 10:e0118889.doi: 10.1371/journal.pone.0118889 [PubMed: 25774892]
24. Johnston MV, Fatemi A, Wilson MA, Northington F. Treatment advances in neonatal neuroprotection and neurointensive care. Lancet Neurol. 2011; 10:372–82. DOI: 10.1016/S1474-4422(11)70016-3 [PubMed: 21435600]
25. Nance E, Porambo M, Zhang F, Mishra MK, Buelow M, Getzenberg R, et al. Systemic dendrimer-drug treatment of ischemia-induced neonatal white matter injury. J Control Release. 2015; 214:112–20. DOI: 10.1016/j.jconrel.2015.07.009 [PubMed: 26184052]
26. Kannan S, Dai H, Navath RS, Balakrishnan B, Jyoti A, Janisse J, et al. Dendrimer-based postnatal therapy for neuroinflammation and cerebral palsy in a rabbit model. Sci Transl Med. 2012; 4:130ra46–130ra46. DOI: 10.1126/scitranslmed.3003162
27. Nakajima W, Ishida A, Lange MS, Gabrielson KL, Wilson M, Martin LJ, et al. Apoptosis has a prolonged role in the neurodegeneration after hypoxic ischemia in the newborn rat. J Neurosci. 2000; 20:7994–8004. doi:20/21/7994. [PubMed: 11050120]
28. Mishra MK, Beaty CA, Lesniak WG, Kambhampati SP, Zhang F, Wilson MA, et al. Dendrimer brain uptake and targeted therapy for brain injury in a large animal model of hypothermic circulatory arrest. ACS Nano. 2014; 8:2134–47. DOI: 10.1021/nn404872e [PubMed: 24499315]
29. Iezzi R, Guru BR, Glybina IV, Mishra MK, Kennedy A, Kannan RM. Dendrimer-based targeted intravitreal therapy for sustained attenuation of neuroinflammation in retinal degeneration. Biomaterials. 2012; 33:979–88. DOI: 10.1016/j.biomaterials.2011.10.010 [PubMed: 22048009]
30. Lesniak WG, Mishra MK, Jyoti A, Balakrishnan B, Zhang F, Nance E, et al. Biodistribution of fluorescently labeled PAMAM dendrimers in neonatal rabbits: Effect of neuroinflammation. Mol Pharm. 2013; 10:4560–71. DOI: 10.1021/mp400371r [PubMed: 24116950]
31. Navath RS, Kurtoglu YE, Wang B, Kannan S, Romero R, Kannan RM. Dendrimer-drug conjugates for tailored intracellular drug release based on glutathione levels. Bioconjug Chem. 2008; 19:2446–55. DOI: 10.1021/bc800342d [PubMed: 19053299]
32. Dai H, Navath RS, Balakrishnan B, Guru BR, Mishra MK, Romero R, et al. Intrinsic targeting of inflammatory cells in the brain by polyamidoamine dendrimers upon subarachnoid administration. Nanomedicine. 2010; 5:1317–29. DOI: 10.2217/nnm.10.89 [PubMed: 21128716]
33. Nance E, Zhang F, Mishra MK, Zhang Z, Kambhampati SP, Kannan RM, et al. Nanoscale effects in dendrimer-mediated targeting of neuroinflammation. Biomaterials. 2016; 101:96–107. DOI: 10.1016/j.biomaterials.2016.05.044 [PubMed: 27267631]

34. Silva SL, Vaz AR, Barateiro A, Falcão AS, Fernandes A, Brito MA, et al. Features of bilirubin-induced reactive microglia: from phagocytosis to inflammation. Neurobiol Dis. 2010; 40:663–75. DOI: 10.1016/j.nbd.2010.08.010 [PubMed: 20727973]
35. Kurpius D, Nolley EP, Dailey ME. Purines induce directed migration and rapid homing of microglia to injured pyramidal neurons in developing hippocampus. Glia. 2007; 55:873–84. DOI: 10.1002/glia [PubMed: 17405148]
36. Woo MS, Wang X, Faustino JV, Derugin N, Wendland MF, Zhou P, et al. Genetic deletion of CD36 enhances injury after acute neonatal stroke. Ann Neurol. 2012; 72:961–70. DOI: 10.1002/ana.23727 [PubMed: 23280844]
37. Perumal OP, Inapagolla R, Kannan S, Kannan RM. The effect of surface functionality on cellular trafficking of dendrimers. Biomaterials. 2008; 29:3469–76. DOI: 10.1016/j.biomaterials.2008.04.038 [PubMed: 18501424]
38. Albertazzi L, Serresi M, Albanese A, Beltram F. Dendrimer internalization and intracellular trafficking in living cells. Mol Pharm. 2010; 7:680–8. DOI: 10.1021/mp9002464 [PubMed: 20394437]
39. Alvarez-Diaz A, Hilario E, Goni de Cerio F, Valls-i-Soler A, Alvarez-Diaz F. Hypoxic-Ischemic Injury in the Immature Brain - Key Vascular and Cellular Players. Neonatology. 2007; 92:227–35. DOI: 10.1159/000103741 [PubMed: 17556841]
40. Barger SW, Goodwin ME, Porter MM, Beggs ML. Glutamate release from activated microglia requires the oxidative burst and lipid peroxidation. J Neurochem. 2007; 101:1205–1213. DOI: 10.1111/j.1471-4159.2007.04487.x [PubMed: 17403030]
41. Zhang F, Nance E, Alnasser Y, Kannan R, Kannan S. Microglial migration and interactions with dendrimer nanoparticles are altered in the presence of neuroinflammation. J Neuroinflamm. 2016; 13:65.doi: 10.1186/s12974-016-0529-3
42. Comi AM, Trescher WH, Abi-Raad R, Johnston MV, Wilson MA. Impact of age and strain on ischemic brain injury and seizures after carotid ligation in immature mice. Int J Devl Neurosci. 2009; 27:271–7. DOI: 10.1016/j.ijdevneu.2008.12.006
43. Sampath D, White AM, Raol YH. Characterization of neonatal seizures in an animal model of hypoxic-ischemic encephalopathy. Epilepsia. 2014; 55:985–93. DOI: 10.1111/epi.12646 [PubMed: 24836645]
44. Clayton EL, Cousin MA. Quantitative monitoring of activity-dependent bulk endocytosis of synaptic vesicle membrane by fluorescent dextran imaging. J Neurosci Methods. 2009; 185:76–81. DOI: 10.1016/j.jneumeth.2009.09.016 [PubMed: 19766140]
45. Liu CL, Siesjo BK, Hu BR. Pathogenesis of hippocampal neuronal death after hypoxia-ischemia changes during brain development. Neuroscience. 2004; 127:113–123. DOI: 10.1016/j.neuroscience.2004.03.062 [PubMed: 15219674]
46. Ness JM, Harvey CR, Washington JD, Roth KA, Carroll SL, Zhang J. Differential activation of c-Fos and caspase-3 in hippocampal neuron subpopulations following neonatal hypoxia-ischemia. J Neurosci Res. 2008; 86:1115–1124. DOI: 10.1002/jnr.21573 [PubMed: 18030677]
47. Bona E, Andersson AL, Blomgren K, Gilland E, Puka-Sundvall M, Gustafson K, et al. Chemokine and inflammatory cell response to hypoxia-ischemia in immature rats. Pediatr Res. 1999; 45:500–9. DOI: 10.1203/00006450-199904010-00008 [PubMed: 10203141]
48. Tortorici MA, Kochanek PM, Poloyac SM. Effects of hypothermia on drug disposition, metabolism, and response: A focus of hypothermia-mediated alterations on the cytochrome P450 enzyme system. Crit Care Med. 2007; 35:2196–204. DOI: 10.1097/01.CCM.0000281517.97507.6E [PubMed: 17855837]
49. Statler KD, Alexander HL, Vagni VA, Nemoto EM, Tofovic SP, Dixon CE, et al. Moderate hypothermia may be detrimental after traumatic brain injury in fentanyl-anesthetized rats. Crit Care Med. 2003; 31:1134–9. DOI: 10.1097/01.CCM.0000054864.43122.52 [PubMed: 12682484]
50. van den Broek MP, Groenendaal F, Egberts AC, Rademaker CM. Effects of hypothermia on pharmacokinetics and pharmacodynamics: A systematic review of preclinical and clinical studies. Clin Pharmacokinet. 2010; 49:277–94. DOI: 10.2165/11319360-000000000-00000 [PubMed: 20384391]

51. Kitchens KM, Kolhatkar RB, Swaan PW, Ghandehari H. Endocytosis inhibitors prevent poly(amidoamine) dendrimer internalization and permeability across caco-2 cells. Mol Pharm. 2008; 5:364–9. DOI: 10.1021/mp700089s [PubMed: 18173246]

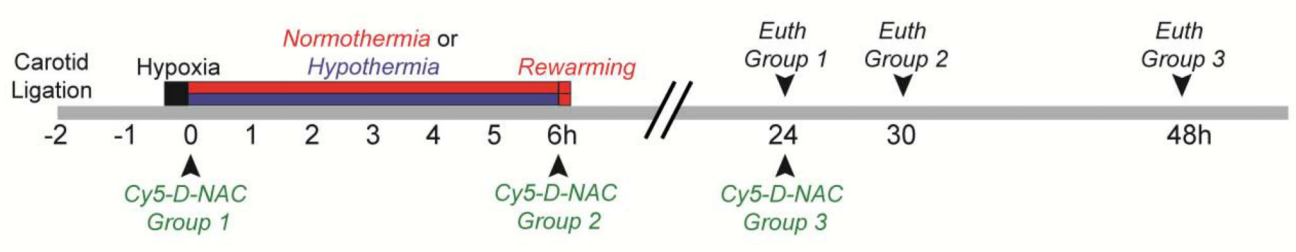

Figure 1. Experimental timeline

CD1 mice underwent permanent unilateral carotid ligation on P7. Pups recovered for 75–90 min before hypoxia (10% O_2 in N_2, 15 min). Immediately following hypoxia, mice were exposed to normothermic or hypothermic conditions and were treated with Cy5-D-NAC 0, 6, or 24 h after HI. Mice were euthanized 24 h after dendrimer administration.

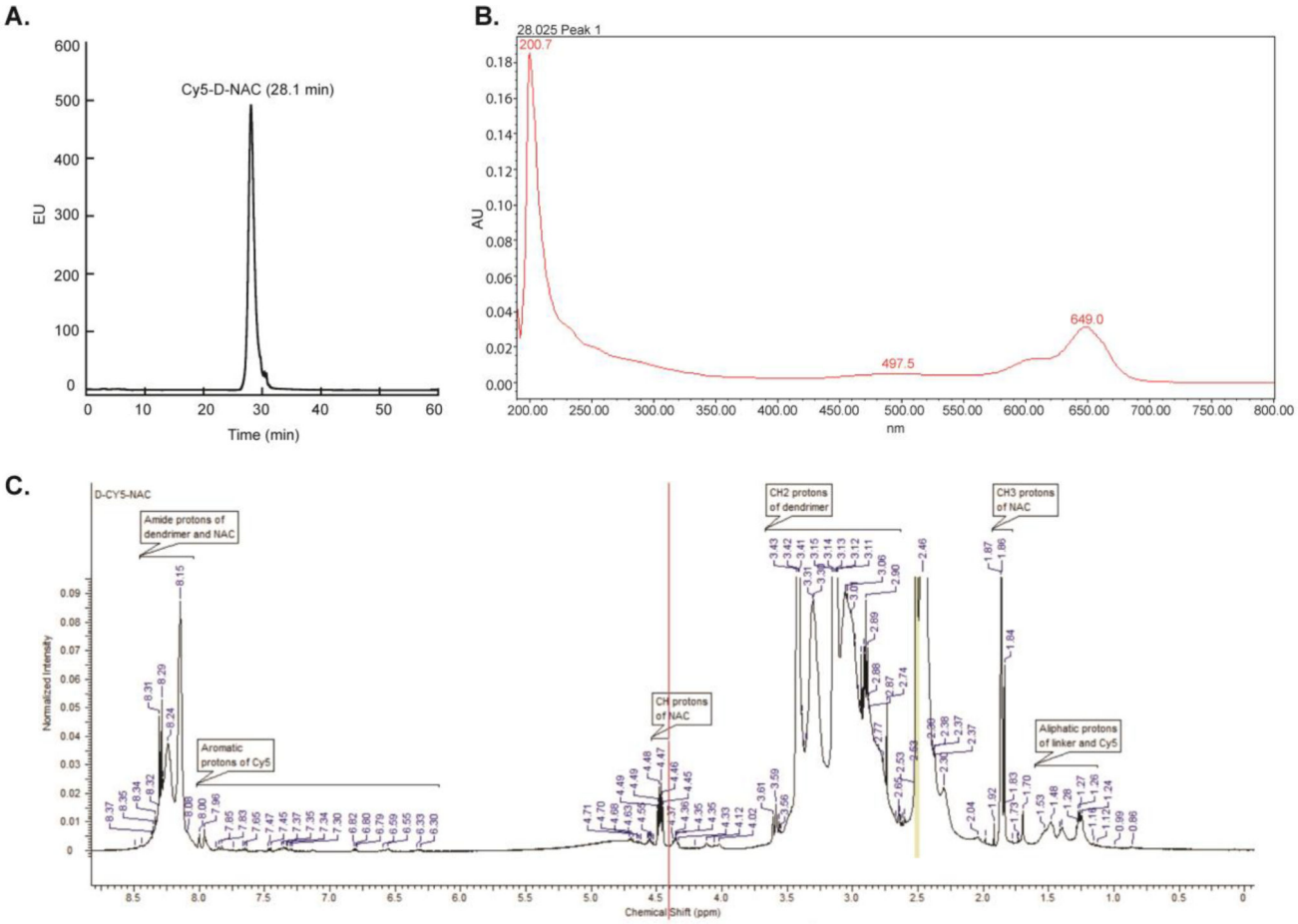

Figure 2. RP-HPLC, UV-vis spectrum, and ^{1}H-NMR characterization of Cy5-D-NAC conjugates

(A) RP-HPLC of Cy5-D-NAC, monitored under fluorescence detector with $\lambda_{excitation}$ = 645 nm, $\lambda_{excitation}$ = 662 nm. The HPLC trace showed a peak at 28.1 min for Cy5-D-NAC, different from that of the starting dendrimer and free Cy5. (B) The UV spectrum showed peaks at 200.7 nm and 649 nm, which are characteristic of PAMAM dendrimer and Cy5. Only one mole equivalent of Cy5 was used in the reaction and the percentage payload of Cy5 to dendrimer is ~4–5%. (C) ^{1}H NMR spectrum of Cy5-D-NAC in DMSO-d_6: δ 1.24–1.53 (m, CH_2 protons of linker and aliphatic protons of Cy5), 1.86 (s, CH_3 protons of NAC), 2.30–3.61 (m, CH_2 protons of G4-OH, SCH_2 protons of NAC and CH_2 protons of SPDP) 4.33–4.49 (m, CH protons of NAC), 6.30–7.85 (m, aromatic protons of Cy5), 7.96–8.31 (m, NHCO protons of G4-OH, amide protons of NAC).

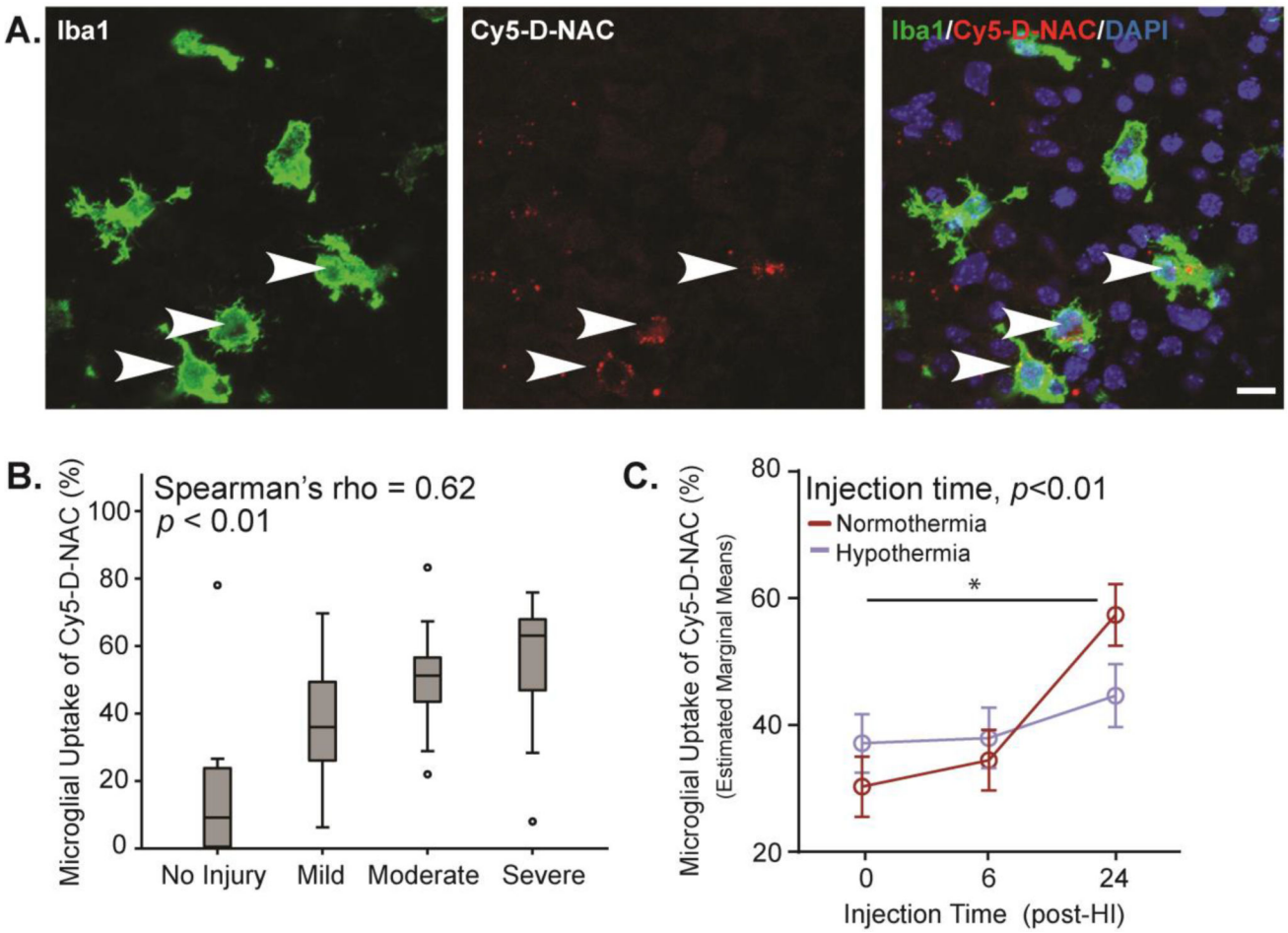

Figure 3. Microglial uptake of Cy5-D-NAC was correlated with injury, increased at 24 h, but was unaffected by hypothermia

(A) Representative images show maximum intensity projections of microglia (Iba1, green), Cy5-D-NAC (red), and nuclei (DAPI, blue) in CA3 within the hippocampus. (B) Uptake of Cy5-D-NAC by microglial cells correlated with the degree of injury (boxplot: box depicts 25^{th} to 75^{th} percentile, Spearman's rho = 0.62; $p < 0.01$). (C) After controlling for the effect of injury using covariate analysis, uptake of dendrimer varied as a function of injection time ($F_{2,71} = 7.16$, $p < 0.01$; figure depicts estimated marginal means ± s.e.m). Bar = 10 μm

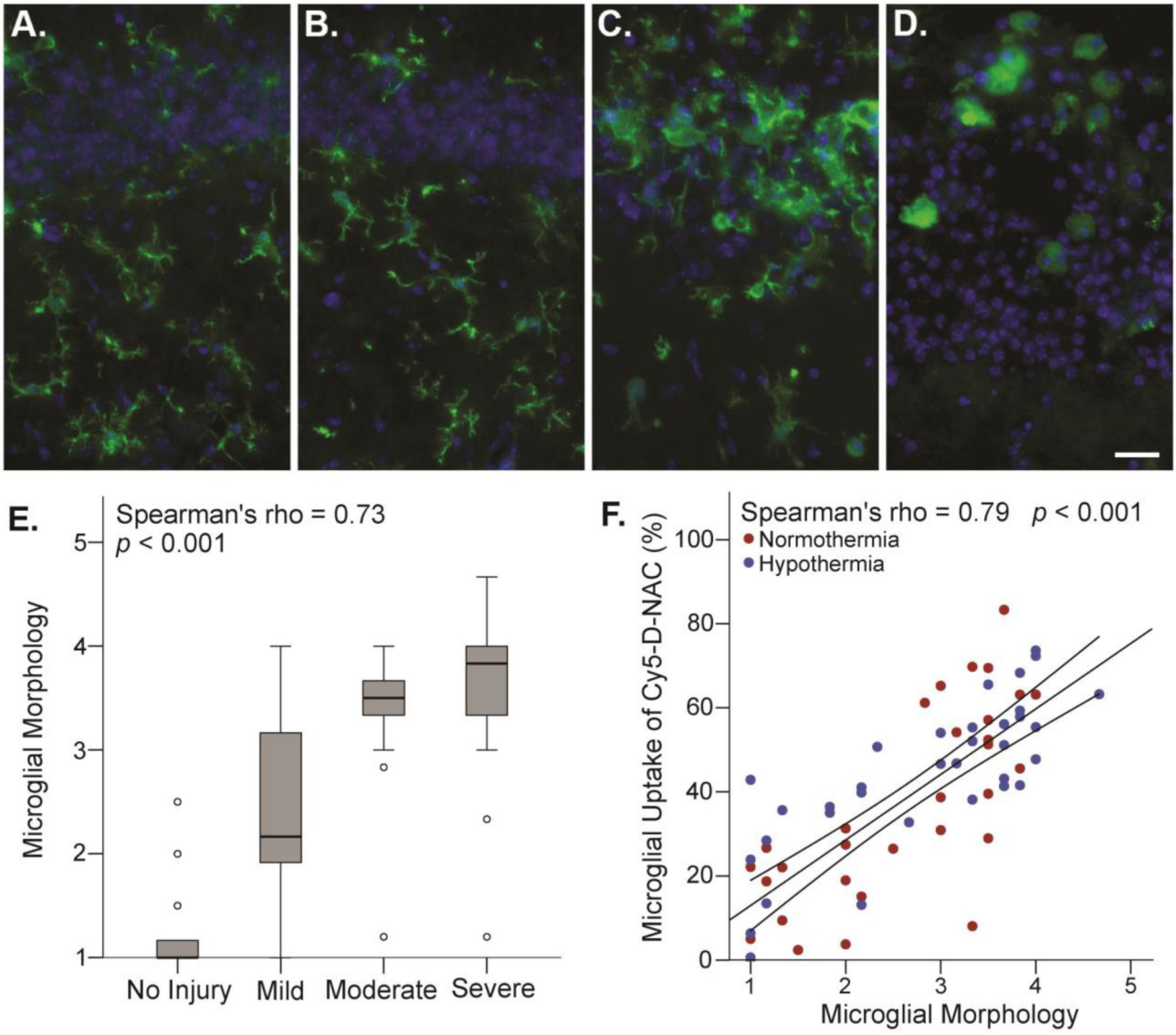

Figure 4. Microglial activation, as indicated by morphology, correlated with brain injury and uptake of Cy5-D-NAC

Microglial morphology was examined in the same images used for uptake analysis and scored as described; CA1 is shown. (A) In uninjured controls, Iba-1-positive microglia (green) exhibited ramified morphology. (B) In a case with mild injury, microglia had a ramified morphology (score = 1). (C) In a case with moderate injury, microglia exhibited moderately activated morphology, with enlarged soma and thickened, often sheet-like processes (score = 3). (D) In a case with severe injury, microglia exhibited highly activated, ameboid morphology (score = 5; blue = DAPI). (E) As expected, microglial morphology scores were correlated with brain injury (boxplot, Spearman's rho = 0.73; $p < 0.001$). (F) Microglial uptake of Cy5-D-NAC was strongly correlated with microglial activation, as indicated by morphology score (Spearman's rho = 0.79, $p < 0.001$; linear regression line with 95% confidence interval for mean). Bar = 20 μm.

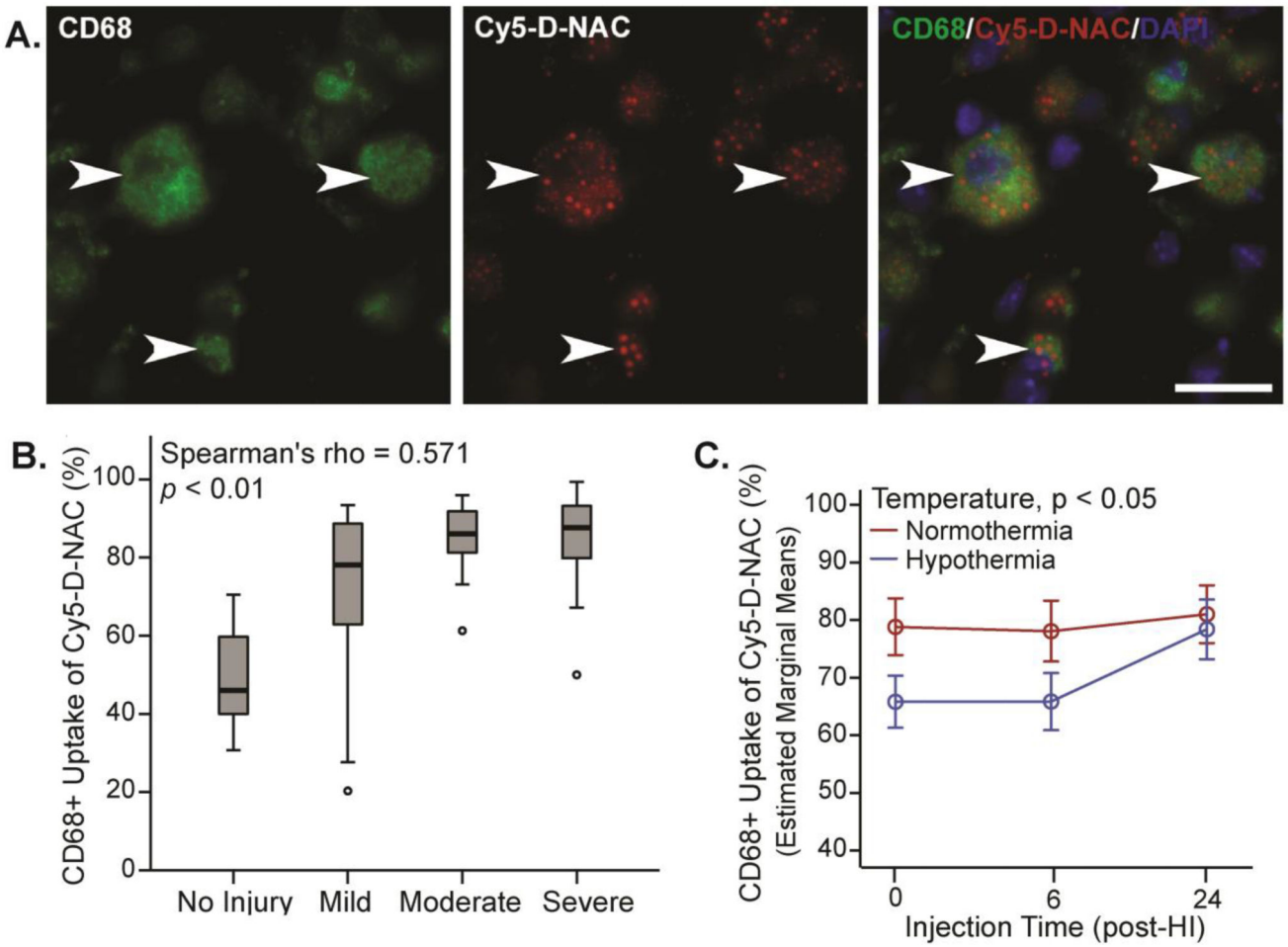

Figure 5. Uptake of Cy5-D-NAC by CD68+ phagocytic microglia was correlated with injury and was reduced by hypothermia

(A) Extended focus images of phagocytic microglia (CD68+, green), Cy5-D-NAC (red), and nuclei (DAPI, blue) in CA3. (B) Cy5-D-NAC uptake by CD68+ microglia correlated with severity of injury (boxplot, Spearman's rho = 0.514, $p < 0.01$). (C) After controlling for the effect of injury using covariate analysis, uptake of Cy5-D-NAC was lower in hypothermic animals ($p < 0.05$; estimated marginal means ± s.e.m). Bar = 20 μm

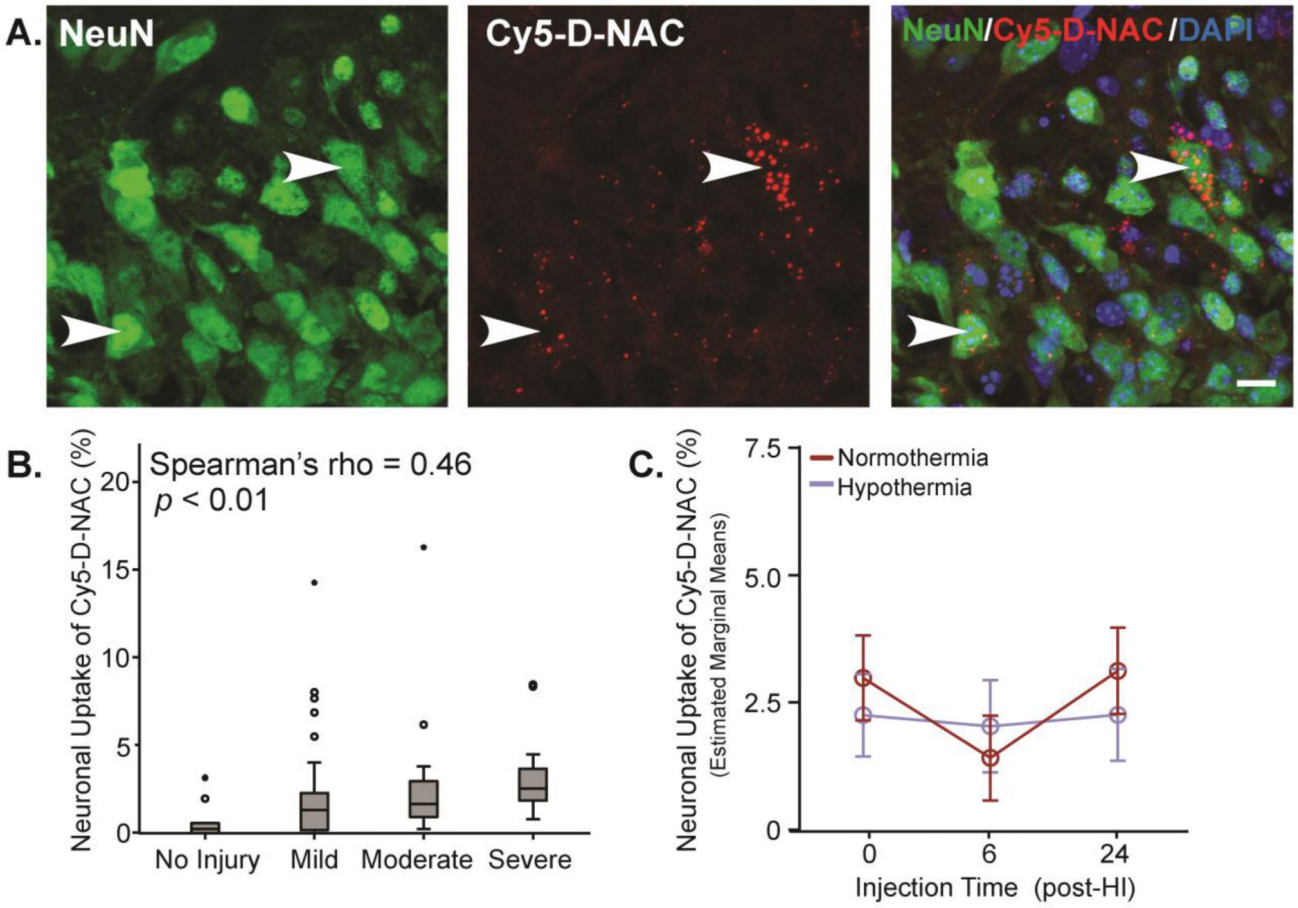

Figure 6. Neuronal uptake of Cy5-D-NAC correlated with injury but was unaffected by hypothermia

(A) Maximum intensity projections of neurons (NeuN, green), Cy5-D-NAC (red), and nuclei (DAPI, blue) in CA1. (B) Cy5-D-NAC uptake by neurons was correlated with injury (boxplot; Spearman's rho = 0.46, $p < 0.01$). (C) When data from the three hippocampal regions were pooled and adjusted for the effect of injury, neuronal uptake of Cy5-D-NAC did not vary as a function of time or temperature (estimated marginal means ± s.e.m.). Bar = 10 μm.

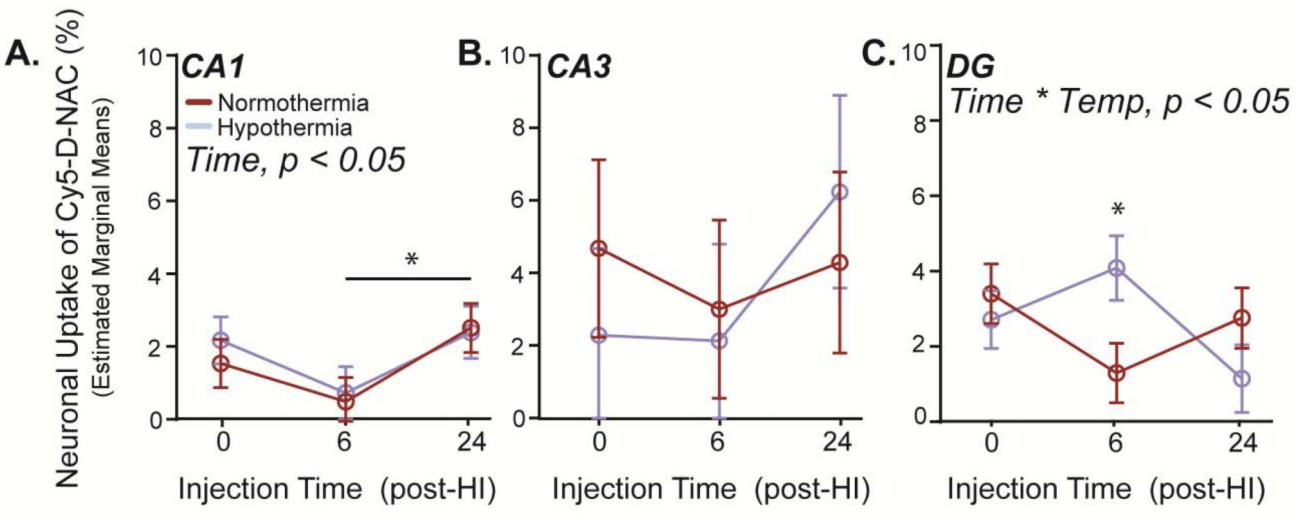

Figure 7. Temporal patterns of neuronal Cy5-D-NAC uptake varied among hippocampal regions, and in DG uptake was greater at the onset of rewarming

(A) In CA1, after adjusting for injury, uptake of the dendrimer varied as a function of time ($p < 0.05$), with decreased uptake in mice injected 6 h after HI. (B) No significant differences in uptake were observed in CA3. (C) In DG, uptake by neurons showed an interaction of injection time and temperature ($p < 0.05$); uptake of Cy5-D-NAC was greater in hypothermic animals when administered 6 h after HI, at the onset of rewarming ($p < 0.05$, estimated marginal means ± s.e.m.).

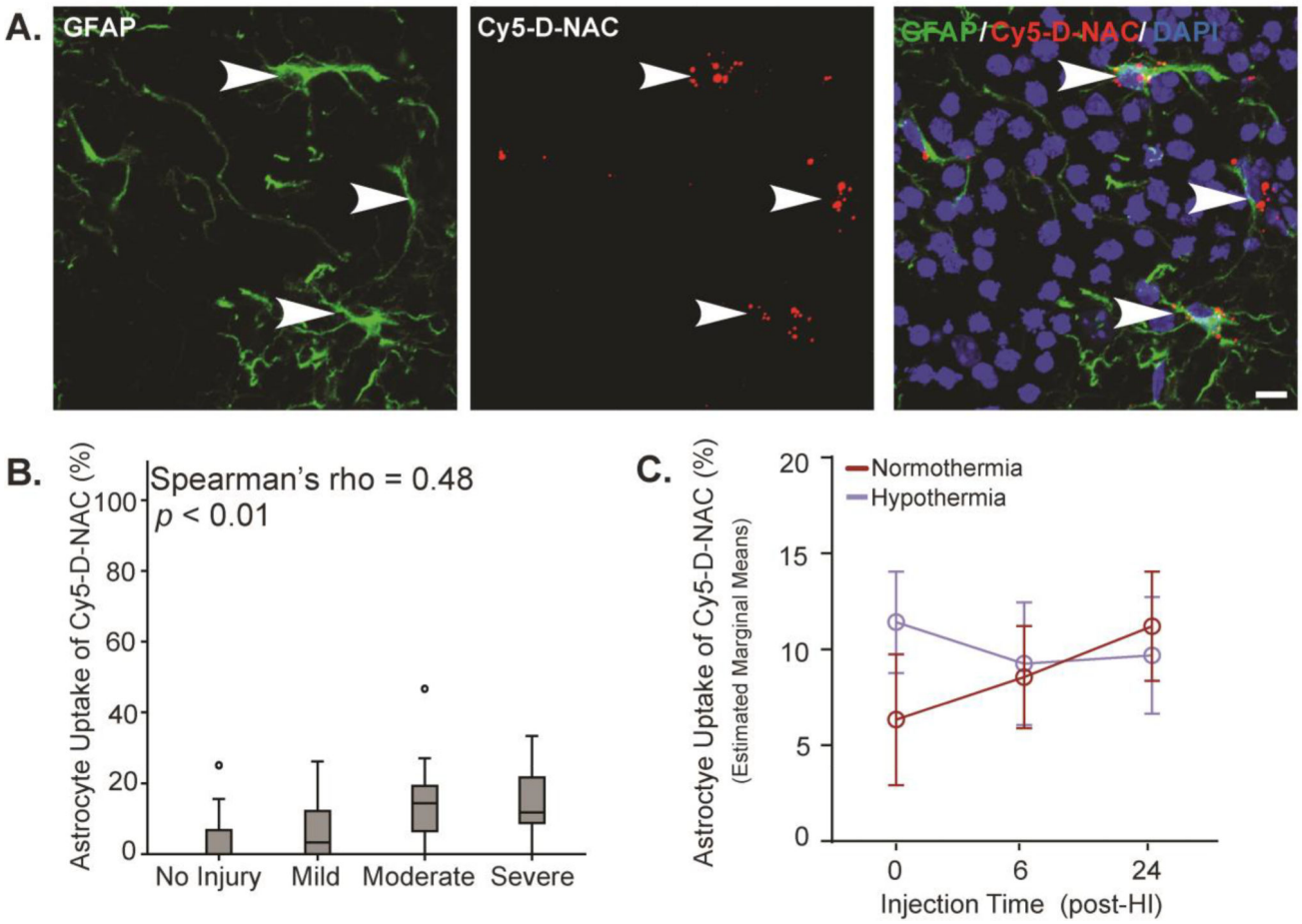

Figure 8. Astrocyte uptake of Cy5-D-NAC correlated with injury but was unaffected by injection time or hypothermia

(A) Maximum intensity projections of astrocytes (GFAP, green), Cy5-D-NAC (red), and nuclei (DAPI, blue) in CA3. (B) Uptake of dendrimer conjugates by astrocytes correlated with injury (boxplot, Spearman's rho = 0.48, $p < 0.01$). (C) When adjusted for injury, uptake by astrocytes did not vary as a function of injection time or hypothermic treatment (estimated marginal means ± s.e.m.). Bar = 10 μm.

Table 1

Distribution of mice among treatment groups. (74 mice survived HI to perfusion, 16% overall mortality, 12 mice served as uninjured controls).

Cy5-D-NAC at:	**0 h**		**6 h**		**24 h**	
	Normothermic	Hypothermic	Normothermic	Hypothermic	Normothermic	Hypothermic
Male	7	6	6	6	6	6
Female	6	7	7	5	6	6